ELSEVIER

Inorganica Chimica Acta 226 (1994) 17–24

Inorganica Chimica Acta

Synthesis, electrochemistry and photoexcited-state properties of dinuclear ruthenium complexes bridged by 2,6′-bis(2-pyridyl)-2,2′:6,2″-thiazolo[4,5-*d*]-benzothiazole

Masa-aki Haga [a,*], Md. Meser Ali [a], Shiro Koseki [a], Akio Yoshimura [b], Koichi Nozaki [b], Takeshi Ohno [b]

[a] *Department of Chemistry, Faculty of Education, Mie University, 1515 Kamihama, Tsu, Mie 514, Japan*

[b] *Department of Chemistry, Faculty of Science, Osaka University, Machikaneyama, Toyonaka, Osaka 560, Japan*

Received 15 April 1994

Abstract

The new bridging ligand, 2,6′-bis(2-pyridyl)-2,2′:6,2″-thiazolo[4,5-*d*]-benzothiazole (bptb) and its dinuclear Ru complexes have been synthesized. The combination of the transient absorption (TA) spectra and spectroelectrochemical difference spectra has led to the assignment of the lowest excited state for the dinuclear Ru(II) complexes as a Ru-to-bptb charge transfer state. Although the ab initio molecular calculations of bridging ligands have provided lower HOMO/LUMO energies for bptb compared to those of 2,6-bis(2-pyridyl)benzodiimidazole (dpimbH_2), the degree of electronic coupling for the dinuclear bptb complex is smaller than that for the dpimbH_2 complex from the analysis of intervalence charge transfer band. Since both dinuclear Ru complexes have a similar coordination environment, the Ru dπ–HOMO Lπ mixing is dominant for the metal–metal interaction through the hole transfer mechanism.

Keywords: Spectroelectrochemistry; Charge transfer excited state; Ruthenium complexes; Dinuclear complexes; Mixed-valence complexes

1. Introduction

There has been increasing interest in dinuclear Ru polypyridine complexes with regard to the understanding of electronic interaction between the metal ions and of photoinduced intramolecular electron/energy transfer reactions [1]. Recently, the supramolecular assemblies consisting of oligonuclear metal complexes with a bridging ligand have been proposed as having potential for photochemical molecular devices [2]. For realizing such supramolecular assemblies, the selection of metal ions, and peripheral and bridging ligands is required. In particular, the separation distance between the two metal ions, the spatial orientation, and the through-bond coupling can be changed by the bridging ligand. Thus, the molecular design of the bridging ligand is important in building up the supramolecular assemblies.

Concerning the electronic structure of the bridging ligand, the orbital mixing between the metal dπ orbitals and the ligand HOMO/LUMO (Lπ or Lπ*) orbitals is discussed from the viewpoint of electron-type or hole-type superexchange mechanisms in the mixed-valence Ru(II)–Ru(III) complexes [3]. In the electron-type superexchange mechanism given in Scheme 1, the mixing between the LUMO π^* orbitals and Ru(II) dπ orbital is the major contribution for metal–metal interaction. On the other hand, the hole-type superexchange mechanism is attributable to an electronic interaction between

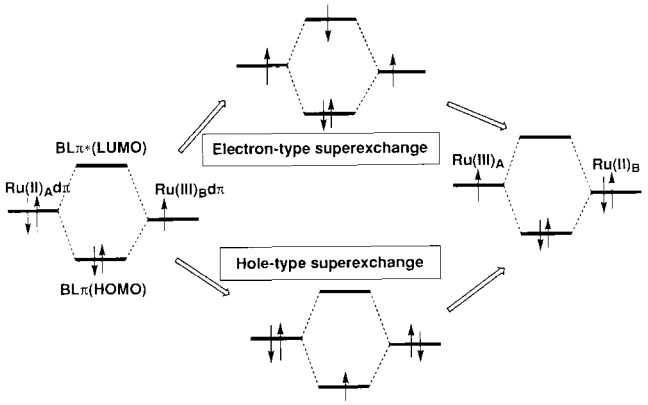

Scheme 1.

* Corresponding author.

SSDI 0020-1693(94)04066-5

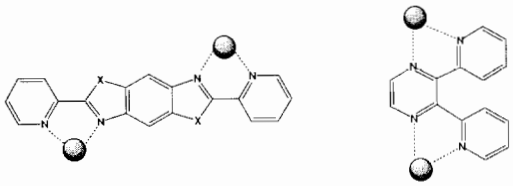

X = NH dpimbH$_2$
S bptb

dpp

Scheme 2. Bridging ligands and their abbreviations.

the HOMO π orbitals of the bridged ligand and Ru(III) dπ orbitals.

Recently, the importance of the hole-transfer mechanism in intervalence charge transfer transition between Ru(II) and Ru(III) has been pointed out in several anionic-type bridging systems such as bibenzimidazolate and 1,2-diacetylhydrazido dianion [3,4a]. In these bridging ligands, the ligand HOMO orbitals are located in relatively high energy, and interact with the Ru dπ orbitals more strongly than the LUMO π^* orbitals do. Thus, the hole-type transfer versus the electron-type transfer mechanism in Ru dinuclear complexes could be controlled by selecting the orbital energies in the bridging ligand.

The benzimidazole fragment has a relatively strong π-donor property, resulting in the stabilization of the Ru(III) state compared to the pyridine or pyrazine fragment [5]. We are continuing our studies on the molecular design of the bridging ligands based on the benzimidazole fragment [4]. In the previous study, we reported the photoexcited property of the dinuclear Ru complex containing 2,6-bis(2-pyridyl)benzodiimidazole (dpimbH$_2$), in which the superexchange interaction was enhanced when the excited electron resided on the bridging dpimbH$_2$ ligand [4e]. As an extension of the previous study, we here report the synthesis and properties of a new bridging ligand, 2,6′-bis(2-pyridyl)-2,2′:6,2″-thiazolo[4,5-*d*]-benzothiazole (bptb), and its Ru dinuclear complex. In the bptb bridging ligand, the N–H imino group of dpimbH$_2$ is substituted by an S atom. For the Ru dinuclear complexes, several examples of sulfur-containing bridging ligands are known, but not extensively [6] (Scheme 2).

2. Experimental

2.1. Materials

2,5-Diamino-1,4-benzenedithiol dihydrochloride (Tokyo Kasei) and 2-picolinic acid (Nacalai) were used as supplied. Tetra-n-butylammonium tetrafluoroborate (TBABF$_4$) was purchased from Nacalai, recrystallized twice from ethyl acetate/pentane, and vacuum dried at 70 °C for 12 h. Acetonitrile was dried over phosphorus pentoxide twice and then distilled over CaH$_2$ under nitrogen. All other chemicals were of analytical grade, and used as supplied.

2.2. Preparations

The perdeuterio 2,2′-bipyridine (bpy-d$_8$) was synthesized according to the literature method [7]. The starting complexes, Ru(bpy)$_2$Cl$_2$·2H$_2$O [8] and Ru(bpy-d$_8$)$_2$Cl$_2$ [7] (bpy = 2,2′-bipyridine, bpy-d$_8$ = perdeuterio 2,2′-bipyridine), were prepared by the literature methods.

Caution! Perchlorate salts are potentially explosive. Although no detonation tendencies have been observed, caution is advised and handling of only small quantities is recommended.

2.2.1. Bridging ligand, 2,6′-bis(2-pyridyl)-2,2′:6,2″-thiazolo[4,5-d]-benzothiazole (bptb)

2,5-Diamino-1,4-benzenedithiol dihydrochloride (3.0 g, 12.2 mmol) in polyphosphoric acid was heated at 90 °C for 15 h, during which time the volume of the contents increased remarkably because of the evolution of hydrogen chloride gas. After the gas evolution ceased, 2-picolinic acid (3.0 g, 24.4 mmol) was added to the resulting yellow solution. The mixture was heated at 150 °C for 16 h. After being cooled to 100 °C, the resulting dark red solution was poured into methanol (500 cm^3). The yellow precipitate was collected and put into an aqueous solution of 2 M ammonia for neutralization. The pale yellow precipitate was collected, washed with water, cthanol, cther and dried in vacuo. Yield 4.3 g. M.p. >270 °C. Mass spectrum: $m/z = 346$ (M^+); $M = C_{18}H_{10}N_4S_2$. *Anal.* Calc. for $C_{18}H_{10}N_4S_2$: C, 62.41; H, 2.91; N, 16.17. Found: C, 61.95; H, 2.72; N, 16.50%.

2.2.2. Dinuclear complexes

$[Ru(bpy)_2(bptb)Ru(bpy)_2](ClO_4)_4 \cdot 4H_2O$. Ru(bpy)$_2Cl_2$ (0.30 g, 0.26 mmol) was dispersed in 30 cm^3 of glycerol and stirred with heating at 100 °C for 1 h. To this dark red solution was added solid bptb (0.15 g, 0.13 mmol), and the solution was heated at 130 °C for an additional 25 h. After cooling, the resulting reaction mixture was diluted with water (20 cm^3) and filtered. To the filtrate was added an aqueous solution of NaClO$_4$ (1.0 g, 8.2 mmol), precipitating the desired complex. The product was filtered, and purified by SP Sephadex C-25 column chromatography with acetonitrile/Britton–Robinson buffer (1:1 vol./vol.) as eluent. The desired dinuclear complex was eluted at pH 9 with 0.05 M sodium chloride as a third dark red–brown band, which was collected, followed by evaporation of the solvent. The dark black residue was recrystallized from methanol/water (5:1 vol./vol.). Yield 0.2 g (39%). *Anal.* Calc. for $C_{58}H_{42}N_{12}O_{16}Cl_4S_2Ru_2 \cdot 4H_2O$: C, 42.40; H, 3.07; N, 10.23. Found. C, 42.71; H, 3.21; N, 10.23%.

$[Ru(bpy\text{-}d_8)_2(bptb)Ru(bpy\text{-}d_8)_2](ClO_4)_4 \cdot 4H_2O$. This complex was similarly obtained from the reaction of $Ru(bpy\text{-}d_8)_2Cl_2$ (0.20 g, 0.4 mmol) with bptb (0.07 g, 0.2 mmol) in glycerol and purified by SP Sephadex C-25 column chromatography with acetonitrile/Britton–Robinson buffer (1:1 vol./vol.; pH 7 with 0.08 M sodium chloride) as eluent. The dark black residue was recrystallized from methanol/acetonitrile (6:1 vol./vol.). Yield 0.1 g (30%). *Anal.* Calc. for $C_{58}H_{42}N_{12}O_{16}Cl_4S_2Ru_2 \cdot 4H_2O$ (for the molecular weight calculation = $C_{58}H_{10}D_{32}N_{12}O_{16}Cl_4S_2Ru_2 \cdot 4H_2O$): C, 41.58; H, 3.01; N, 10.03. Found: C, 41.93; H, 3.14; N, 10.08%.

2.3. Physical measurements

Electronic spectra were obtained on a Hitachi U-3210 spectrophotometer from 200 to 850 nm and a Hitachi 3400 spectrophotometer from 800 to 2600 nm. Fourier transform NMR spectra were recorded on a JEOL-GX270 spectrometer. Electrochemical measurements were made at 20 °C with a BAS 100/W electrochemical analyzer. The working electrode was a glassy-carbon or platinum electrode and the auxiliary electrode was a platinum plate. The reference electrode was a BAS RE-1 Ag/AgCl electrode. All the potentials are referred to those of the ferrocenium/ferrocene ($Fc^{+/0}$) couple, which is +0.33 V versus SCE. The spectroelectrochemistry was performed by using a platinum minigrid (80 mesh) working electrode in the thin-layer cell. The cell was located directly in the spectrophotometer, and the absorption change was monitored during the electrolysis. The flow electrolysis was performed by the same flow-through cell as reported previously [5d]. In the flow controlled potential electrolysis, the current at a set potential is directly proportional to the number of electrons used during the oxidation. The plot of current versus absorbance at one wavelength gives the oxidative titration curve. For the intervalence charge transfer band in the mixed-valence complex, the comproportionation constant can be determined by the analysis of this titration curve [9].

An Hitachi spectrofluorometer, model MPF-2A was used to obtain the emission spectra at room temperature. Emission lifetimes were measured by means of the single-photon-counting methods on a Horiba NASE-550 nanosecond fluorometer system. The sample was excited by the 500 nm pulses from a hydrogen gas lamp through a Nikon G-50 monochromator. Transient absorption spectra after exposure to the second harmonic pulse of the Q-switched Nd^{3+}-YAG laser were obtained by the procedure described in Ref. [10]. The geometrical structures of the bridging ligands bptb and $dpimbH_2$ were optimized using the STO-3G basis set [11] within Hartree–Fock approximation (HF/STO-3G). The HF/3-21G method [12] was employed to obtain more reliable electronic structures at the HF/STO-3G optimized geometries. All calculations were performed using the quantum chemistry program code GAMESS [13].

3. Results and discussion

3.1. Characterization

The synthetic route for the bridging ligand and complexes is summarized in Scheme 3. The bptb bridging ligand was obtained by the condensation reaction of 2,5-diamino-1,4-benzenedithiol dihydrochloride with 2 equiv. of 2-picolinic acid in polyphosphoric acid. This ligand is insoluble in all the solvents. The stoichiometric reaction between $Ru(L)_2Cl_2$ (L = bpy, bpy-d_8) and bptb (2:1 molar ratio) in glycerol gave the dinuclear complex, $[Ru(L)_2(bptb)Ru(L)_2]^{4+}$. However, even when the reaction was run in a 1:1 molar ratio, only the dinuclear complex was formed. The synthesis of the mononuclear complex is currently under way. The dinuclear complex is soluble in polar solvents such as acetonitrile and acetone. The bis bidentate coordination fashion of bptb was confirmed by the ^1H NMR Spectra of $[Ru(bpy\text{-}d_8)_2(bptb)Ru(bpy\text{-}d_8)_2](ClO_4)_4 \cdot 4H_2O$ in DMSO-d_6, which are shown in Fig. 1.

The ^1H NMR spectra of $[Ru(bpy\text{-}d_8)_2(bptb)Ru(bpy\text{-}d_8)_2](ClO_4)_4 \cdot 4H_2O$ consist of five sets of signals together with other small signals. By comparison with the reported chemical shifts of related benzimidazole complexes [14] and spin–spin coupling constants, the signals can be assigned to H(3), H(4), H(6), H(5), H(α) protons in this order from the low frequency signal. The singlet feature of the H(α) proton indicates the magnetically symmetric environment in the bptb bridging ligand. When the bptb ligand forms a symmetrical bis bidentate

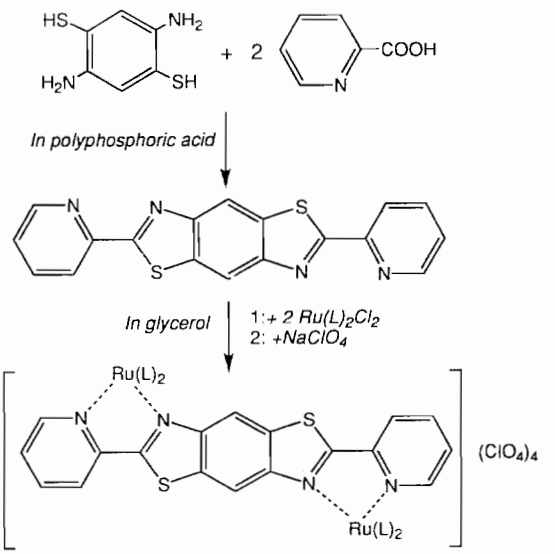

Scheme 3.

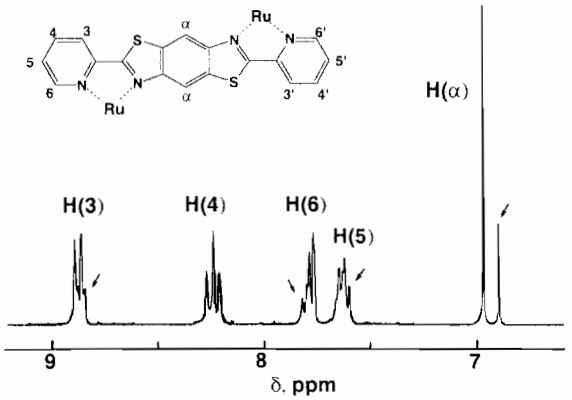

Fig. 1. ^{1}H NMR spectra of $[Ru(bpy\text{-}d_8)_2(bptb)Ru(bpy\text{-}d_8)_2](ClO_4)_4 \cdot 4H_2O$ in DMSO-d_6.

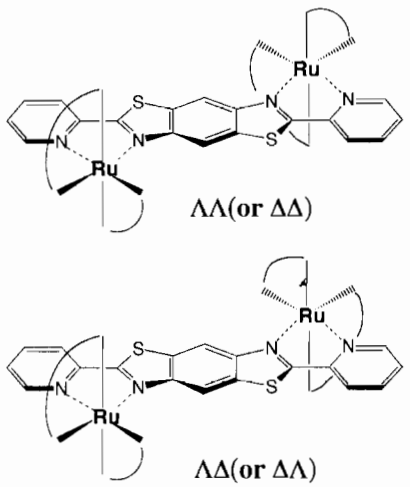

Scheme 4.

coordination, two coordination fashions are possible; i.e. two N–N or two N–S coordination. If the complex has a two N–S coordination mode, free imino nitrogens would exist and the protonation reaction on the free N sites would be expected. Since there is no UV spectral change on the addition of perchloric acid into the dinuclear bptb complex in CH_3CN, no free imino nitrogens exist. Consequently, the bptb bridging ligand is coordinated to two $Ru(bpy)_2$ moieties through the two N–N bidentate fashion. Two groups of ^{1}H NMR signals with an intensity ratio of 3:1 in Fig. 1 suggest the existence of diastereoisomers in the solution, as shown in Scheme 4 but with a different ratio. Recently, the separation of pure stereoisomers has been reported, in which the larger shielding for the protons in $\Delta\Delta/\Lambda\Lambda$ complexes compared to the $\Delta\Lambda/\Lambda\Delta$ ones were observed on the ^{1}H NMR spectra because of the ring current induced by the adjacent ring [15]. In the present complex, the H(α) protons show the most significant difference of the chemical shifts between the two stereoisomers: the minor portion of the stereoisomers appears at a higher field compared to the major portion. Considering the interligand through-space ring current anisotropy, the major portion in the stereoisomers can be assigned to the $\Delta\Lambda/\Lambda\Delta$ diastereoisomer.

3.2. Electrochemistry

The cyclic voltammogram of $[Ru(bpy)_2(bptb)Ru(bpy)_2]^{4+}$ in CH_3CN is shown in Fig. 2. One oxidation process labeled I and three reduction processes II, III, IV are observed. Oxidative process I is chemically reversible, and coulometry results show that two electrons are involved in this process. The peak-to-peak separation is 65 mV. Following the analysis of this peak-to-peak separation by Richardson and Taube [16], process I consists of two closely spaced one-electron processes with potentials, $E_{1/2}{}^1 = 0.96$ and $E_{1/2}{}^2 = 1.00$ V versus $Fc^{+/0}$.

$$[Ru(II)\text{–}bptb\text{–}Ru(II)]^{4+} \overset{E^0{}_1}{\rightleftharpoons} [Ru(III)\text{–}bptb\text{–}Ru(II)]^{5+} \overset{E^0{}_2}{\rightleftharpoons} [Ru(III)\text{–}bptb\text{–}Ru(III)]^{6+}$$

$$\Delta E_{1/2} = E^0{}_2 - E^0{}_1$$

Furthermore, the separation between two oxidation potentials is 40 mV for $[Ru(bpy)_2(bptb)Ru(bpy)_2]^{4+}$, which is smaller than the reported value (80 mV) for $[Ru(bpy)_2(dpimbH_2)Ru(bpy)_2]^{4+}$ [4e]. This potential separation is thermodynamically related to the equilibrium constant, K_{com}, for the comproportionation as shown below [17]:

$$[Ru(II)\text{–}BL\text{–}Ru(II)]^{4+} + [Ru(III)\text{–}BL\text{–}Ru(III)]^{6+} \rightleftharpoons 2[Ru(II)\text{–}BL\text{–}Ru(III)]^{5+}$$

BL = bptb, $dpimbH_2$

By using the thermodynamic relationship between the potential separation and comproportionation constant, the value $K_{com} = 4.7$ is obtained for the present system. A small K_{com} for $[Ru(bpy)_2(bptb)Ru(bpy)_2]^{4+}$

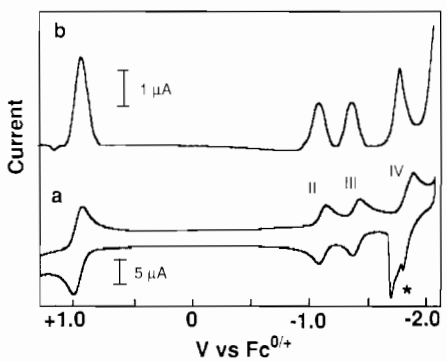

Fig. 2. Cyclic voltammogram of $[Ru(bpy)_2(bptb)Ru(bpy)_2]^{4+}$ (0.5 mM) in CH_3CN (0.1 M $TBABF_4$) at a platinum electrode at room temperature. Scan rate = 100 mV s^{-1}.

indicates the instability of the mixed-valence Ru(II)–Ru(III) state for the bptb system.

On the other hand, both reduction processes II and III are one-electron processes at −1.13 and −1.41 V, while process IV at $E_{pc} = -1.90$ V is complicated by an absorption to the electrode, but the peak height on differential pulse voltammogram (DPV) suggests two electrons may be involved. The oxidation process is Ru(II)/Ru(III) metal based, while the reduction processes are associated with the ligand π^* LUMO energies. By comparison with the reduction potentials of $[Ru(bpy)_3]^{2+}$ and $[Ru(bpy)_2(L)]^{2+}$ [4a], the reduction processes II and III are bridging ligand bptb based and process IV is peripheral bpy based as shown in Scheme 5. Thus, the LUMO in this dinuclear complex consists of mainly bridging ligand bptb π^* orbitals.

The oxidation potential for $[Ru(bpy)_2(bptb)Ru(bpy)_2]^{4+}$ ($E_{1/2}^1 = 0.96$ and $E_{1/2}^2 = 1.00$ V versus $Fc^{+/0}$) is higher than that for $[Ru(bpy)_2(dpimbH_2)Ru(bpy)_2]^{4+}$ [4e], suggesting that the bptb bridging ligand is a stronger π acceptor than $dpimbH_2$. This stronger π acceptor property can be supported by the lower reduction potentials in $[Ru(bpy)_2(bptb)Ru(bpy)_2]^{4+}$.

3.3. Absorption and emission spectra

Absorption spectra of $[Ru(bpy)_2(bptb)Ru(bpy)_2]^{4+}$ in CH_3CN are shown in Fig. 3, and the spectral data are collected in Table 1 together with analogous Ru complexes. The absorption bands at 516 and 435 nm correspond to Ru dπ-to-π^*(bptb) and Ru dπ-to-π^*(bpy) metal-to-ligand charge-transfer (MLCT) transitions, respectively. The intense π–π^*(bptb) intraligand band appears at 384 and 364 nm. Changing the bridging ligands in the dinuclear complexes, $[Ru(bpy)_2(BL)Ru(bpy)_2]^{4+}$, shifts the MLCT band maximum to a lower energy in the order of $BL = dpimbH_2 < bptb < dpp$. These results indicate that the π-acceptor property for the bridging ligand BL increases in this order.

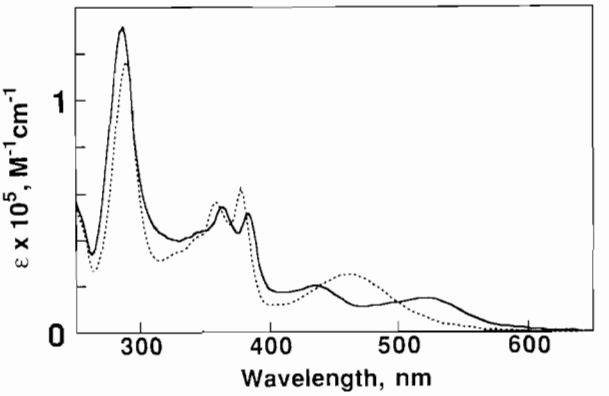

Fig. 3. Absorption spectra of $[Ru(bpy)_2(BL)Ru(bpy)_2]^{4+}$ in CH_3CN. BL = bptb is shown as a solid line and $dpimbH_2$ as a dotted line.

The complex, $[Ru(bpy)_2(bptb)Ru(bpy)_2]^{4+}$, in CH_3CN exhibits an emission maximum at 746 nm (uncorrected) with a lifetime of 115 ns at room temperature. Since the energy of emission decreases on going from the $dpimbH_2$ bridged complex to the bptb one, the energy gap between the Ru dπ and Lπ^* orbitals decreases. As a result, the lifetime of the excited state decreases, followed by the energy gap law [18].

The spectroelectrochemical oxidation of $[Ru(bpy)_2(bptb)Ru(bpy)_2]^{4+}$ in CH_3CN at +1.2 V versus $Fc^{+/0}$ leads to a complete loss of the MLCT band at 516 and 435 nm and the appearance of a new ligand-to-Ru(III) charge transfer (LMCT) band with low intensity at 764 nm after the two-electron oxidation (Fig. 4). After the complete oxidation, the original spectra can be regenerated by reduction at +0.5 V.

3.4. Transient absorption (TA) spectra

Fig. 5 shows a TA spectrum of $[Ru(bpy)_2(bptb)Ru(bpy)_2]^{4+}$ in CH_3CN at room temperature immediately after laser excitation. A characteristic feature of the TA spectrum is a bleaching of the π–π^* band of bptb at 364 and 384 nm and an enhancement at 420 nm and around 750 nm. This TA spectrum is quite different from that of $[Ru(bpy)_3]^{2+}$ [4c,19], but quite similar to that of $[Ru(bpy)_2(dpimbH_2)Ru(bpy)_2]^{4+}$ reported previously, although the peaks and valleys showed longer wavelength shifts [4e]. A comparison between the TA spectrum and the spectra of the oxidized and reduced form of $[Ru(bpy)_2(bptb)Ru(bpy)_2]^{4+}$ is informative. The electrochemical two-electron oxidation of $[Ru(bpy)_2(bptb)Ru(bpy)_2]^{4+}$ gave rise to a difference absorption spectrum with reference to that of the Ru(II) compound, as shown in Fig. 6(a). The one-electron

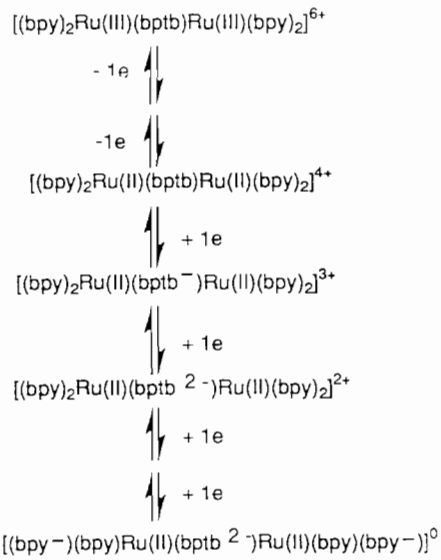

Scheme 5.

Table 1
Spectral and electrochemical data

Complex	Absorption		Emission	Redox potentials	
	λ_{max} (nm) (ϵ (M^{-1} cm^{-1}))	Assignment	λ_{max} (nm) (lifetime (ns))	vs. $Fc^{+/0}$ (V)	Redox site
$[Ru(bpy)_2(bptb)Ru(bpy)_2]^{4+}$	285 (129000)	bpy(π–π^*)	746 (115)	oxidation	
	364 (53800)	BL(π–π^*)		0.96, 1.00	Ru(II/III)
	384 (51100)	BL(π–π^*)		reduction	
	435 (13000)	MLCT		−1.13	BLbptb
	516 (14300)	MLCT		−1.42	BLbptb
				−1.90	bpy
$[Ru(bpy)_2(dpimbH_2)Ru(bpy)_2]^{4+}$ [a]	288 (116000)	bpy(π–π^*)	680 (606)	oxidation	
	359 (57600)	BL(π–π^*)		0.75, 0.83	Ru(II/III)
	378 (62400)	BL(π–π^*)		reduction	
	461 (24900)	MLCT		−1.79(E_{pc})irr	
				−1.88	bpy
				−2.17	bpy
$[Ru(bpy)_2(dpp)Ru(bpy)_2]^{4+}$ [b]	284 (115000)	bpy(π–π^*)	802 (125)	oxidation	
	425 (19800)	MLCT		0.99, 1.16	Ru(II/III)
	526 (24700)	MLCT		reduction	
				−1.05	dpp
				−1.55	dpp
				−1.95	bpy

[a]Ref. [4e].
[b]Ref. [19].

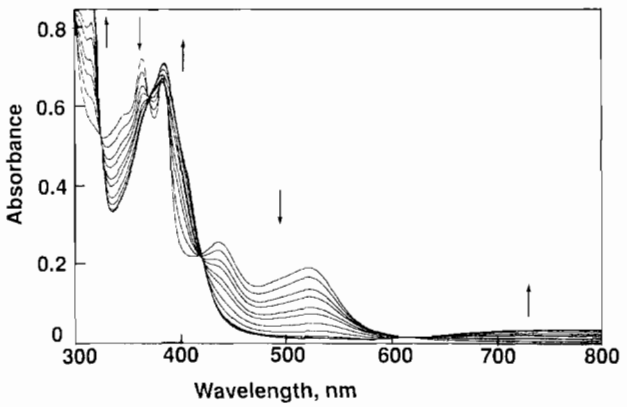

Fig. 4. Time resolved absorption spectra of $[Ru(bpy)_2(bptb)Ru(bpy)_2]^{4+}$ (0.26 mM) in CH_3CN (0.1 M $TBABF_4$) on the spectroelectrochemical oxidative condition at +1.2 V vs. $Fc^{+/0}$.

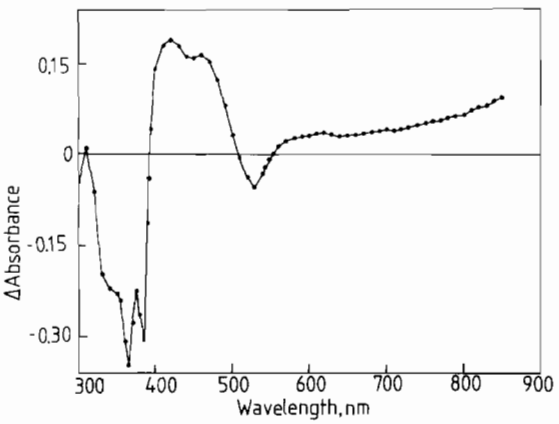

Fig. 5. Transient absorption (TA) spectrum of $[Ru(bpy)_2(bptb)Ru(bpy)_2]^{4+}$ (0.1 mM) in CH_3CN at room temperature immediately after laser excitation.

oxidized difference spectra of $[Ru(bpy)_2(bptb)Ru(bpy)_2]^{4+}$ was calculated as half of this fully oxidized difference spectrum. The negative bands of the difference spectrum at 435 and 516 nm correspond to the bleaching of the MLCT bands. The positive bands are seen at 398 and 316 nm in the difference absorption spectrum, which can be assigned as a bptb π–π^* and a bpy π–π^* band coordinated to Ru(III) ion, respectively. A positive band around 750 nm is assigned to bptb-to-Ru(III) charge transfer and bpy-to-Ru(III) charge transfer (LMCT), as in the case of $[Ru(bpy)_3]^{2+}$ and $[Ru(bpy)_2(bpbimH_2)]^{2+}$ ($bpbimH_2$ = 2,2′-bis(2-pyridyl)bibenzimidazole) [4c,4d]. Similarly, the difference spectrum on electrochemical reduction at −1.3 V provides a positive band at 469 nm and negative bands at 384, 364 and 314 nm (Fig. 6(b)). By comparing the TA spectrum with the electrochemical difference absorption spectra, the strong bleaching of the π–π^* transition of bptb at 364 and 384 nm indicates the reduction of the bptb bridging ligand, and the enhancement of the band at 420 nm and around 750 nm is assigned to the π–π^* band of $bptb^-$. These data strongly indicate that the excited electron resides on the bptb bridging ligand.

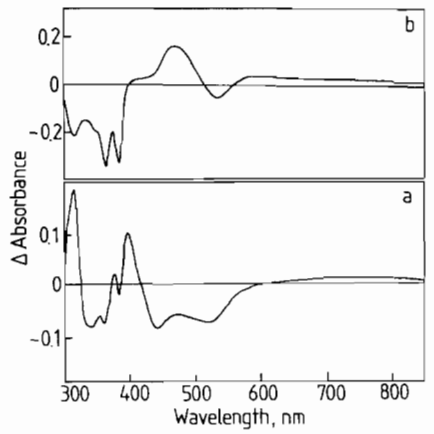

Fig. 6. Difference absorption spectra of $[Ru(bpy)_2(bptb)Ru(bpy)_2]^{4+}$ (0.26 mM) in CH_3CN (0.1 M $TBABF_4$) on the spectroelectrochemical condition: (a) half of the spectrum obtained by the oxidation at +1.2 V, (b) the reduction at −1.3 V vs. $Fc^{+/0}$.

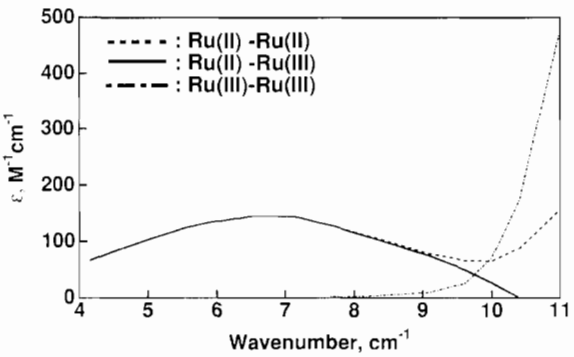

Fig. 7. The intervalence charge transfer band of $[Ru(bpy)_2(bptb)Ru(bpy)_2]^{4+}$ in CH_3CN, obtained by the flow oxidative electrolysis. The spectra were corrected by considering the comproportionation equilibrium.

$$[Ru(II)(bptb)Ru(II)]^{4+} \xrightarrow{h\nu} [Ru(III)(bptb^{-})Ru(II)]^{4+*}$$

3.5. Metal–metal interaction in the dinuclear complexes

While the original complex, $[Ru(bpy)_2(bptb)Ru(bpy)_2]^{4+}$, is transparent in the near-IR region (> 700 nm), the flow oxidative controlled-electrolysis exhibits a new broad band at 1490 nm (6700 cm^{-1}) on the edge of the LMCT band at 750 nm, which can be assigned to an IT transition. This assignment is confirmed by the disappearance of this band when the potential is set under the fully oxidation condition of the dinuclear complex (Fig. 7). The degree of electronic coupling between the metal centers, H_{AB}, can be evaluated from the position, bandwidth and intensity of the IT band using the following equation [17,20]:

$$H_{AB} = 2.05 \times 10^{-2} \left[\frac{\epsilon_{max} \Delta\nu_{1/2}}{\nu_{max}}\right]^{1/2} \left[\frac{\nu_{max}}{r}\right] \quad (\text{in } cm^{-1})$$

where ϵ_{max} is the extinction coefficient (in $M^{-1}\,cm^{-1}$), ν_{max} is the wavenumber of the IT absorption maximum (in cm^{-1}), $\Delta\nu_{1/2}$ is the bandwidth at half-intensity (in cm^{-1}), and r is the distance between the metal sites (in Å). For the bptb dinuclear complex, the value of the Ru–Ru distance $r = 8$ Å was used on the basis of the molecular model. The observed bandwidth (4570 cm^{-1}) is a little broader than the calculated one (3930 cm^{-1}). The H_{AB} value for the bptb system is estimated to be 180 cm^{-1}, which is smaller than that for $dpimbH_2$ (470 cm^{-1}).

In order to shed light on the electronic structure of the bptb ligand, ab initio molecular orbital calculations of bptb and $dpimbH_2$ were carried out. The HOMO and LUMO energies for bptb are −8.362 and 1.216 eV, while those for $dpimbH_2$ are −7.529 and 1.744 eV, respectively. From these MO calculations, the HOMO and LUMO energies for bptb are lower than those for $dpimbH_2$. Furthermore, the π orbitals on the ligand are seen in both HOMO and LUMO (Fig. 8), which can be interacted with the Ru dπ orbitals. By comparing the H_{AB} value for the bptb complex with that for $dpimbH_2$, a smaller value of H_{AB} is obtained for the bptb complex. The metal–metal interaction in the mixed-valence complexes would be dependent on the overlap between the frontier orbitals of the metal and the bridging ligand, which is determined by the energy gap between the metal dπ orbitals and the LUMO and HOMO orbitals of the bridging ligand. By comparison with the analogous bridging systems, the lowering of the HOMO/LUMO energies should lead to a larger overlap between the Ru dπ orbitals and the LUMO, on the other hand the raising of the HOMO/LUMO energies causes a larger overlap between the Ru dπ orbitals and the HOMO (see Fig. 8) [3a]. Considering the similar coordination environment between the bptb and $dpimbH_2$ complexes, the overlap between the Ru dπ orbitals and the HOMO determines the strength of the metal–metal interaction in the present systems, and consequently the hole-type transfer mech-

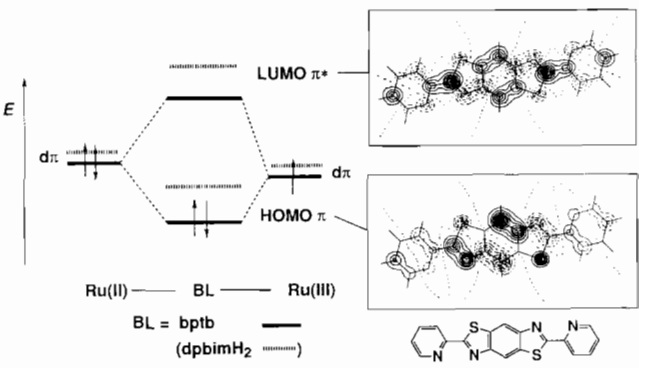

Fig. 8. Schematic presentation of the orbital mixing between the HOMO/LUMO of the bridging ligand (BL) and two Ru dπ orbitals. The contour plots of the HOMO/LUMO of bptb are shown as an inset. Dashed lines indicates regions of negative phase.

anism becomes a dominant superexchange pathway. When the bptb complex is photochemically excited, the negative charge on the bridging ligand of the excited electron may enhance the hole-type superexchange interaction between the metal sites.

Acknowledgements

M.H. gratefully acknowledges financial supports from the Ministry of Education for a Grant-in-Aid for Scientific Research (No. 04453045 and 06804036), the Sumitomo Foundation for a basic science grant, and the Japan Securities Scholarship Foundation. M.M.A. also thanks the Ministry of Education for a Japanese Government (Monbusho) Scholarship.

References

[1] (a) T. Ohno, *Prog. React. Kinet., 14* (1988) 219; (b) F. Scandola, C.A. Bignozzi, C. Chiorboli, M.T. Indelli and M.A. Rampi, *Coord. Chem. Rev., 97* (1990) 299–312; (c) J.D. Petersen, in V. Balzani (ed.), *Supramolecular Photochemistry,* Reidel, Dordrecht, Netherlands, 1987, p. 135; (d) J.-M. Lehn, p. 29; (e) C.A. Bignozzi, S. Roffia, C. Chiorboli, J. Davila, M.T. Indelli and F. Scandola, *Inorg. Chem., 28* (1989) 4350; (f) D.P. Rillema, R.W. Callahan and K.B. Mack, *Inorg. Chem., 21* (1982) 2589; (g) S. Ernst and W. Kaim, *Inorg. Chem., 28* (1989) 1520; (h) L. De Cola, P. Belser, F. Ebmeyer, F. Barigelletti, F. Vogtle, A. von Zelewsky and V. Balzani, *Inorg. Chem., 29* (1990) 495; (i) R. Hage, A.H.J. Dijkhuis, J.G. Haasnoot, R. Prins, J. Reedijk, B.E. Buchana and J.G. Vos, *Inorg. Chem., 27* (1988) 2185; (j) J.R. Shaw, R.T. Webb and R.H. Schmehl, *J. Am. Chem. Soc., 112* (1990) 1117; (k) K.S. Schanze, G.A. Neyhart and T.J. Meyer, *J. Phys. Chem., 90* (1986) 2182; (l) J.C. Curtis, J.S. Bernstein and T.J. Meyer, *Inorg. Chem., 24* (1985) 385; (m) W.E. Jones, Jr., S.M. Baxter, G.F. Strouse and T.J. Meyer, *J. Am. Chem. Soc., 115* (1993) 7363; (n) V. Balzani and F. Scandola, in M.A. Fox and M. Chanon (eds.), *Photoinduced Electron Transfer. Part D,* Elsevier, New York, 1988, p. 148; (o) W.R. Murphy, K.J. Brewer, G. Gettliffe and J.D. Petersen, *Inorg. Chem., 28* (1989) 81; (p) M.Y. Ogawa, J.F. Wishart, Z. Young, J.R. Moller and S.S. Isied, *J. Phys. Chem., 97* (1993) 11456; (q) Y. Fuchs, S. Lofters, T. Dieter, W. Shi, R. Morgan, T.C. Strekas, H.D. Gafney and A.D. Baker, *J. Am. Chem. Soc., 109* (1987) 2691; (r) M. Hunziger and A. Ludi, *J. Am. Chem. Soc., 99* (1977) 7370; (s) E.H. Yonemoto, R.L. Riley, Y.I. Kim, S.J. Atherton, R.H. Schmehl and T.E. Mallouk, *J. Am. Chem. Soc., 114* (1992) 8081; (t) L. De Cola, V. Balzani, F. Barigelletti, L. Flamigni, P. Belser, A. von Zelewsky, M. Frank and F. Vogtle, *Inorg. Chem., 32* (1993) 5228; (u) M.N. Paddon-Row, *Acc. Chem. Res., 27* (1994) 18; (v) Y. Wang, B.T. Hauser, M.M. Rooney, R.D. Burton and K.S. Schanze, *J. Am. Chem. Soc., 115* (1993) 5675.

[2] (a) V. Balzani, L. Moggi and F. Scandola, in V. Balzani (ed.), *Supramolecular Photochemistry,* Reidel, Dordrecht, Netherlands, 1987, p. 1; (b) V. Balzani and F. Scandola, *Supramolecular Photochemistry,* Ellis Horwood, Chichester, UK, 1991; (c) S. Woitellier, J.P. Launay and C.W. Spangler, *Inorg. Chem., 28* (1989) 758; (d) J.P. Launay, in F.L. Carter (ed.), *Molecular Electronic Devices II,* Marcel Dekker, New York, 1987, p. 39; (e) J.J. Hopfield, J.N. Onuchic and D.N. Beratan, *Science, 241* (1988) 817; (f) J.-M. Lehn, *Angew. Chem., Int. Ed. Engl., 27* (1988) 89.

[3] (A) W. Kaim and V. Kasack, *Inorg. Chem., 29* (1990) 4696–4699; (b) J.T. Hupp, *J. Am. Chem. Soc., 112* (1990) 1563; (c) R. Hage, J.G. Haasnoot, H.A. Nieuwenhuis, J. Reedijk, D.J.A. De Ridder and J.G. Vos, *J. Am. Chem. Soc., 112* (1990) 9245–9251.

[4] (a) M. Haga, T. Matsumura-Inoue and S. Yamabe, *Inorg. Chem., 26* (1987) 4148; (b) M. Haga, T. Ano, K. Kano and S. Yamabe, *Inorg. Chem., 30* (1991) 3843–3849; (c) T. Ohno, K. Nozaki, N. Ikeda and M. Haga, *Electron Transfer in Inorganic, Organic and Biological Systems,* Advances in Chemistry, Vol. 228, American Chemical Society, Washington, DC, 1991, p. 215; (d) T. Ohno, K. Nozaki and M. Haga, *Inorg. Chem., 31* (1992) 548–555; (e) *31* (1992) 4256–4261; (f) K. Nozaki, T. Ohno and M. Haga, *J. Phys. Chem., 96* (1992) 10880–10888; (g) M.Haga, T. Ano, T. Ishizaki, K. Kano, K. Nozaki and T. Ohno, *J. Chem. Soc., Dalton Trans.,* (1994) 263–272.

[5] E.C. Constable and P.J. Steel, *Coord. Chem. Rev., 93* (1989) 205.

[6] (a) C.A. Stein and H. Taube, *J. Am. Chem. Soc., 100* (1978) 1635; (b) V. Palaniappan, S. Sathaiah, H.D. Bist and U.C. Agarwala, *J. Am. Chem. Soc., 110* (1988) 6403; (c) M.A. Greaney, C.L. Coyle, M.A. Harmer, A. Jordan and E.I. Stiefel, *Inorg. Chem., 28* (1989) 912.

[7] S. Chirayil and R.P. Thummel, *Inorg. Chem., 28* (1989) 813.

[8] P.A. Lay, A. Sargeson and H. Taube, *Inorg. Synth., 24* (1986) 291.

[9] (a) J.E. Sutton, P.M. Sutton and H. Taube, *Inorg. Chem., 18* (1979) 1017; (b) K. Nozaki, T. Ohno and M. Haga, manuscript in preparation.

[10] T. Ohno, A. Yoshimura and N. Mataga, *J. Phys. Chem., 94* (1990) 4871–4876.

[11] (a) W.J. Hehre, R.F. Stewart and J.A. Pople, *J. Chem. Phys., 51* (1969); (b) W.J. Hehre, R. Ditchfield, R.F. Stewart and J.A. Pople, *J. Chem. Phys., 52* (1970) 2769.

[12] J.S. Binkley, J.A. Pople and W.J. Hehre, *J. Am. Chem. Soc., 102* (1980) 939.

[13] M.W. Schmidt, K.K. Baldridge, J.A. Boatz, S.T. Elbert, M.S. Gordon, J.H. Jensen, S. Koseki, N. Matsunaga, K.A. Nguyen, S. Su, T.L. Windus, M. Dupuis and J.A. Montgomery, Jr., *J. Comput. Chem., 14* (1993) 1347.

[14] (a) X. Xiaoming, M. Haga, T. Matsumura-Inoue, Y. Ru, A.W. Addison and K. Kano, *J. Chem. Soc., Dalton Trans.,* (1993) 2477; (b) P.J. Steel and E.C. Constable, *J. Chem. Soc., Dalton Trans.,* (1990) 1389; (c) M. Haga, *Inorg. Chim. Acta, 77* (1983) L39–41.

[15] (a) X. Hua and A. von Zelewsky, *Inorg. Chem., 30* (1991) 3796; (b) D.A. Reistma and F.R. Keene, *J. Chem. Soc., Dalton Trans.,* (1993) 2859.

[16] D.E. Richardson and H. Taube, *Inorg. Chem., 20* (1981) 1278–1285.

[17] C. Creutz, *Prog. Inorg. Chem., 30* (1983) 1.

[18] T.J. Meyer, *Prog. Inorg. Chem., 30* (1983) 389.

[19] K. Miedler and P.K. Das, *J. Am. Chem. Soc., 104* (1982) 7462.

[20] N.S. Hush, *Prog. Inorg. Chem., 8* (1967) 391.